Proceedings of the XII International Symposium on Dynamic Problems of Mechanics (DINAME 2007),
Varoto, P. S. and Trindade, M. A. (Editors), ABCM, Ilhabela, SP, Brazil, February 26 - March 2, 2007

Nonlinear Dynamics of Fluid-Filled Functionally Graded Cylindrical Shell

P. B. Gonçalves[1], F. M A. Silva[1] and Z. J. G. N del Prado[2]

[1] Civil Engineering Department, Catholic University, PUC - Rio, 22453-900, Rio de Janeiro, RJ, Brazil.

paulo@civ.puc-rio.br, silvafma@yahoo.com.br

[2] Civil Engineering Department ,UFG, 74605-200, Goiânia, GO, Brazil.

zenon@eec.ufg.br

Abstract: The concept of functionally graded materials (FGMs) was first introduced in Japan. Many FGMs are compositionally graded from refractory ceramic to a metal. This type of material may be an ideal choice for shells containing or surrounded by a hot fluid. In this paper the non-linear equations of motion of a functionally graded cylindrical shell are derived based on the von-Karmàn-Donnell nonlinear kinematic relations. The FGMs properties at any point along the shell thickness are a function of the relative volume fraction of metal and ceramic and temperature. They are considered to vary smoothly and continuously along the shell thickness. The fluid is considered to be non-viscous and incompressible and its irrotational motion is described by a velocity potential which must satisfy the Laplace equation. First, the free vibration analysis of the fluid-filled shell is carried out and the influence of the shell and fluid properties on the natural frequencies and vibration modes is evaluated. Based on these results, a low dimensional model is derived for the free and forced nonlinear vibration analysis of shell. The influence of the material and geometrical shells parameters on its nonlinear vibrations are analyzed in detail.

Keywords: cylindrical shells, fluid-structure interaction, parametric instability, dynamic buckling, functionally graded materials.

INTRODUCTION

Functionally graded materials (FGM) have received much attention as an advanced class of non-homogeneous materials with several applications in engineering. The conception of FGM was proposed in 1984 by Japanese scientists with the objective of building effective thermal barriers (Koizumi, 1997). This new class of material is particularly suited for plates and shells. Since 1999 several researches were conducted to study the vibrations and stability of plates and shells made of FGM. As an example, Loy et. al. (1999) analyzed the free vibrations of simply supported cylindrical shells with FGM. In this analysis the linear theory of Love was used for the shell and different exponential functions were used to describe the variation of the materials along the shell thickness. The influence of the materials gradation on the vibration modes was evaluated. Pradhan et al. (2000) extended the work of Loy et al. (1999) to other boundary conditions. Ng et al (2001), using Bolotin's method, studied the dynamic instability of simply-supported cylindrical shells using several gradation laws. Silva et. al. (2006) studied the natural frequencies of a fluid filled cylindrical shell with graded material. The influence of the fluid height on the natural frequencies was evaluated, as well as the effects of the free surface of the fluid, by using the modified Donnell shell equations.

In this paper the non-linear equations of motion of a functionally graded shell cylindrical shell are derived based on the von-Karmàn-Donnell nonlinear kinematic relations. The FGMs properties at any point along the shell thickness are a function of the relative volume fraction of metal and ceramic and temperature. They are considered to vary smoothly and continuously along the shell thickness. The fluid is considered to be non-viscous and incompressible and its irrotational motion is described by a velocity potential which must satisfy the Laplace equation. First, the free vibration analysis of the fluid-filled shell is carried out and the influence of the shell and fluid properties on the natural frequencies and vibration modes is evaluated. Based on these results a low dimensional model is derived for the free and forced nonlinear vibration analysis of shell. The influence of the material and geometrical shells parameters on its nonlinear vibrations is analyzed. To the authors knowledge this is the first work on nonlinear vibrations and instabilities of functionally graded cylindrical shells in literature.

PROBLEM FORMULATION

Functionally graded material

As an example, it is considered that the shell is built with a functionally graded material composed of nickel and silicon nitride, the amount of each material varying according to a given law through its thickness, with silicon nitride in the inner part and nickel in the outer part, as illustrated in Fig. 1.

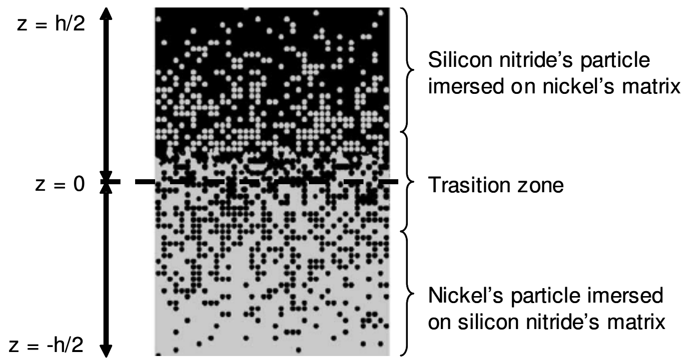

Figure 1 – Gradation of the material through the thickness of the shell.

The variation of nickel volume through the thickness of the shell is assumed as:

$$V_{Ni} = \left(\frac{z}{h} + \frac{1}{2}\right)^{N} \tag{1}$$

where V_{Ni} is the nickel volume. Then, when z = h/2 the nickel volume is maximum, and when, z = -h/2, the silicon nitride volume is maximum. Fig. 2 shows the variation of nickel volume through the shell's thickness for different values of the exponent *N*.

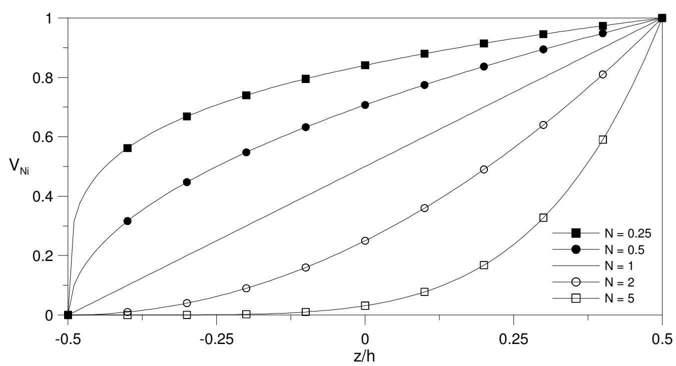

Figure 2 – Variation of nickel volume through shell's thickness.

It is possible to establish a variation for the physical and mechanical properties from Eq. (1) as:

$$\begin{aligned} E &= (E_{Ni} - E_{SN})V_{Ni} + E_{SN} \\ \nu &= (\nu_{Ni} - \nu_{SN})V_{Ni} + \nu_{SN} \\ \rho &= (\rho_{Ni} - \rho_{SN})V_{Ni} + \rho_{SN} \end{aligned} \tag{2}$$

where E, ν, ρ, are, respectively, the modulus of elasticity, Poisson ratio and density of the graded material.

The physical properties of the material can be expressed as a function of the temperature in a polynomial form as (Sofiyev, 2005):

$$P = P_0\left(P_{-1}T^{-1} + 1 + P_1 T + P_2 T^2 + P_3 T^3\right) \tag{3}$$

where P is the intended physical property; P_0, P_{-1}, P_1, P_2 e P_3 are coefficients that relate the dependency of the evaluated property on the temperature, and, T is the absolute temperature in Kelvin. Thus the material properties can be written as a function of the temperature.

Shell equations

Consider a perfect thin-walled circular cylindrical shell of radius R, length L and thickness h. The axial, circumferential and radial co-ordinates are denoted by, respectively, x, y and z, and the corresponding displacements on the shell middle surface are in turn denoted by u, v and w, as shown in Figure 3.

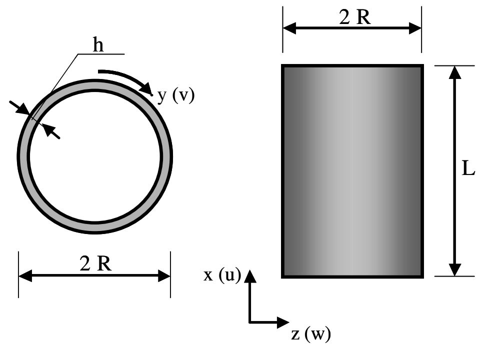

Figure 3 – Geometry and coordinate system of the shell.

The shell is subject to an axial load of intensity $P(t)$ per unit length uniformly applied along the edges of the form:

$$P(t) = P_0 + P_1 \cos(\omega t) \tag{4}$$

where P_0 is the static load, P_1 is the amplitude of the time-dependent load and ω is the forcing frequency.

The non-linear equations of motion based on Donnell shallow shell theory are given by:

$$\begin{aligned}
&\frac{\partial}{\partial x} N_x + \frac{\partial}{\partial y} N_{xy} = 0 \\
&\frac{\partial}{\partial x} N_{xy} + \frac{\partial}{\partial y} N_y = 0 \\
&\rho_1 \frac{\partial^2}{\partial t^2} w + \beta_1 \frac{\partial}{\partial t} w + \beta_2 \nabla^4 \frac{\partial}{\partial t} w - \frac{\partial^2}{\partial x^2} M_x - 2\frac{\partial^2}{\partial x \partial y} M_{xy} - \frac{\partial^2}{\partial y^2} M_y = p_h + (N_x - P(t)) \frac{\partial^2}{\partial x^2} w \\
&+ N_y \left(\frac{\partial^2}{\partial y^2} w - \frac{1}{R} \right) + 2 N_{xy} \frac{\partial^2}{\partial x \partial y} w
\end{aligned} \tag{5}$$

where ∇^4 is the bi-harmonic operator and p_h is the fluid hydrodynamic pressure due to the motions of the shell wall.

The damping coefficients, β_1 e β_2 and the equivalent shell mass density ρ_1 are:

$$\beta_1 = 2\xi \rho_1 \omega_0 \qquad \beta_2 = \eta \frac{E_{SN} h^3}{12 - 12\nu_{SN}^2} \qquad \rho_1 = \int_{-h/2}^{h/2} \rho \, dz \tag{6}$$

The membrane and bending internal forces for a functionally graded shell, appearing in equation (5), are given in terms of the middle-surface strains by:

$$\begin{Bmatrix} N_x \\ N_y \\ N_{xy} \\ M_x \\ M_y \\ M_{xy} \end{Bmatrix} = \begin{bmatrix} A_{11} & A_{12} & 0 & B_{11} & B_{12} & 0 \\ A_{12} & A_{22} & 0 & B_{12} & B_{22} & 0 \\ 0 & 0 & A_{66} & 0 & 0 & B_{66} \\ B_{11} & B_{12} & 0 & C_{11} & C_{12} & 0 \\ B_{12} & B_{22} & 0 & C_{12} & C_{22} & 0 \\ 0 & 0 & B_{66} & 0 & 0 & C_{66} \end{bmatrix} \begin{Bmatrix} \varepsilon_x \\ \varepsilon_y \\ \gamma_{xy} \\ \kappa_x \\ \kappa_y \\ \kappa_{xy} \end{Bmatrix} \tag{7}$$

where the coefficients A_{ij}, B_{ij} e C_{ij} (i,j = 1,2,6), obtained from the constitutive relations are given in Appendix A.

The middle-surface strain-displacement relations and the changes of curvature on which the Donnell equations are based are defined by:

$$\varepsilon_x = \frac{\partial}{\partial x}u + \frac{1}{2}\left(\frac{\partial}{\partial x}w\right)^2 \qquad \kappa_x = -\frac{\partial^2}{\partial x^2}w$$
$$\varepsilon_y = \frac{\partial}{\partial y}v + \frac{w}{R} + \frac{1}{2}\left(\frac{\partial}{\partial y}w\right)^2 \qquad \kappa_y = -\frac{\partial^2}{\partial y^2}w \tag{8}$$
$$\gamma_{xy} = \frac{\partial}{\partial y}u + \frac{\partial}{\partial x}v + \frac{\partial}{\partial x}w\frac{\partial}{\partial y}w \qquad \kappa_{xy} = -2\frac{\partial^2}{\partial x \partial y}w$$

Determination of the displacement field u, v e w

The numerical model is developed by expanding the transversal displacement component *w* in series in the circumferential and axial variables. From previous investigations on modal solutions for the non-linear analysis of cylindrical shells under axial loads (Hunt et al. 1986; Gonçalves and Batista, 1988; Gonçalves and Del Prado, 2002) it is observed that, in order to obtain a consistent modeling with a limited number of modes, the sum of shape functions for the displacements must express the non-linear coupling between the modes and describe consistently the unstable post-buckling response of the shell as well as the correct frequency-amplitude relation.

The lateral deflection *w* can be generally described as (Gonçalves and Batista, 1988):

$$w = \sum_{i=1,3,5}\ \sum_{j=1,3,5} \zeta_{ij}(t)h\cos\left(in\frac{y}{R}\right)\sin\left(jm\pi\frac{x}{L}\right) + \sum_{k=0,2,4}\ \sum_{l=0,2,4} \zeta_{kl}(t)h\cos\left(kn\frac{y}{R}\right)\sin\left(lm\pi\frac{x}{L}\right) \tag{9}$$

where *n* is the number of waves in the circumferential direction of the basic buckling or vibration mode, *m* is the number of half-waves in the axial direction and $\zeta_{ij}(t)$ are the time dependent vibration amplitudes.

These modes represent both the symmetric and asymmetric components of the shell deflection pattern. The first double series represents the unsymmetrical modes with odd multiples of the basic wave numbers *m* and *n*. The second double series represents, besides the asymmetric modes which contains an even multiple of the basic wave numbers *m* and *n* and rosette modes, the axi-symmetric modes which play an important role in the non-linear modal coupling and loss of stability of the shell.

To obtain a low-dimensional model capable of satisfying the necessary boundary, continuity and symmetry conditions, the following modal expansion, obtained from Eq. (9), is adopted for *w*:

$$w = \zeta_{00}(t)h + \zeta_{11}(t)h\sin\left(\frac{m\pi x}{L}\right)\cos\left(\frac{ny}{R}\right) + \zeta_{02}(t)h\cos\left(\frac{2m\pi x}{L}\right) + \zeta_{20}(t)\cos\left(\frac{2ny}{R}\right) \tag{10}$$

In order to solve Eqs. (5) for a functionally graded shell, it is first necessary to derive the displacements *u* and *v* compatible with this modal expansion for *w*.

Consider a stress function *f* defined by the relations:

$$\frac{\partial^2}{\partial y^2}f = N_x \qquad \frac{\partial^2}{\partial x^2}f = N_y \qquad \frac{\partial^2}{\partial x \partial y}f = -N_{xy} \tag{11}$$

which satisfy the in plane equilibrium equations in (5).

Using the well-known compatibility equation

$$\frac{\partial^2}{\partial y^2}\varepsilon_x + \frac{\partial^2}{\partial x^2}\varepsilon_y - \frac{\partial^2}{\partial x \partial y}\gamma_{xy} = 0 \tag{12}$$

together with equations (8) and (11), the following compatibility equation is obtained in terms of *f* and *w* for a functionally graded cylindrical shell:

$$
\begin{aligned}
&\frac{\partial^4}{\partial x^4} f + \frac{\left(A_{11}^2 - 2A_{12}A_{66} - A_{12}^2\right)}{A_{11}A_{66}} \frac{\partial^4}{\partial x^2 \partial y^2} f + \frac{\partial^4}{\partial y^4} f = \frac{\left(A_{11}B_{12} - B_{11}A_{12}\right)}{A_{11}} \frac{\partial^4}{\partial x^4} w \\
&+ \frac{2\left[\left(A_{11}^2 - A_{12}^2\right)B_{66} + \left(A_{12}B_{12} - A_{11}B_{11}\right)A_{66}\right]}{A_{11}A_{66}} \frac{\partial^4}{\partial x^2 \partial y^2} w + \frac{\left(A_{12}B_{11} - A_{11}B_{12}\right)}{A_{11}} \frac{\partial^4}{\partial y^4} w \\
&+ \frac{\left(A_{11}^2 - A_{12}^2\right)}{A_{11}} \left[\left(\frac{\partial^2}{\partial x \partial y} w\right)^2 + \frac{1}{R}\frac{\partial^2}{\partial x^2} w - \frac{\partial^2}{\partial x^2} w \frac{\partial^2}{\partial y^2} w\right]
\end{aligned}
\tag{13}
$$

From equations (11) and (8) the following derivatives of the in-plane displacements u and v are obtained:

$$
\begin{aligned}
\frac{\partial}{\partial x} u = \frac{1}{A_{11}^2 - A_{12}^2} &\left[A_{11}\frac{\partial^2}{\partial y^2} f - A_{12}\frac{\partial^2}{\partial x^2} f + \left(A_{11}B_{11} - A_{12}B_{12}\right)\frac{\partial^2}{\partial x^2} w \right. \\
&\left. + \left(A_{11}B_{12} - A_{12}B_{11}\right)\frac{\partial^2}{\partial y^2} w\right] - \frac{1}{2}\left(\frac{\partial}{\partial x} w\right)^2
\end{aligned}
\tag{14}
$$

$$
\begin{aligned}
\frac{\partial}{\partial y} v = \frac{1}{A_{11}^2 - A_{12}^2} &\left[A_{11}\frac{\partial^2}{\partial x^2} f - A_{12}\frac{\partial^2}{\partial y^2} f + \left(A_{11}B_{12} - A_{12}B_{11}\right)\frac{\partial^2}{\partial x^2} w \right. \\
&\left. + \left(A_{11}B_{11} - A_{12}B_{12}\right)\frac{\partial^2}{\partial y^2} w\right] - \frac{w}{R} - \frac{1}{2}\left(\frac{\partial}{\partial y} w\right)^2
\end{aligned}
\tag{15}
$$

The right hand side of these differential equations are written in terms of w and f. Substituting (10) into (13) and solving the compatibility equation analytically, f can be obtained in terms of the modal amplitudes of w. Substituting the modal expansions for w and f into equations (14) and (15) and solving the resulting differential equation, the displacements u and v are finally obtained in terms of the modal amplitudes of w. The in-plane boundary conditions are

$$
N_x = 0 \quad and \qquad v = 0 \qquad at\ x = 0, L
\tag{16}
$$

They are satisfied "on the average", following the procedure by Amabili et. al. (2003).

The symmetry condition

$$
u = 0 \qquad at\ x = L/2
\tag{17}
$$

is satisfied by the solution of equation (14).

Finally substituting u, v and w into the third equation in (5) (out-of-plane equilibrium equation), and applying the Galerkin method, a set of two non-linear differential equations of motion in terms of the modal are obtained and solved by the Runge-Kutta integration method. Bifurcation diagrams are obtained by the brute-force method.

Fluid Equations

The shell is assumed to be completely filled with an incompressible and non-viscous fluid. The irrotational motion of the fluid can be described by a velocity potential $\phi(x, r, \theta, t)$. This potential function must satisfy the Laplace equation which can be written in dimensionless form as:

$$
\bar{\phi}_{,\xi\xi} + \frac{1}{\kappa}\bar{\phi}_{,\kappa} + \frac{1}{\kappa^2}\bar{\phi}_{,\theta\theta} + \bar{\phi}_{,\kappa\kappa} = 0
\tag{18}
$$

where:

$$
\kappa = r/R \qquad \bar{\phi} = \gamma\phi/R^2 \qquad \gamma = [\rho_s R^2(1-\nu^2)/E]^{1/2}
$$

The dynamic fluid pressure acting on the shell surface is obtained from the Bernoulli equation:

$$
p_h = -\left(\frac{\rho_F}{\rho_S}\right)\left(\frac{\gamma}{4\delta^2}\right)\bar{\phi}_{,t}
\tag{19}
$$

where ρ_F is the density of the fluid and ρ_S is the shell material density.

At the shell-fluid interface, the fluid velocity normal to the shell surface must be equal to the shell velocity in this direction, that is:

$$\bar{\phi}_{,\kappa} = 2\gamma\delta(\partial w/\partial t) \tag{20}$$

where $\delta = h/2R$.

Further, for a fluid-filled shell, the following restriction must be imposed at $\kappa = 0$:

$$\bar{\phi}_{,\kappa} = 0 \tag{21}$$

Solving equations (17) to (20), one obtains the following expressions for the hydrodynamic fluid pressure:

$$p_h = \frac{\partial^2}{\partial t^2}\zeta_{11}(t)\, m_a \cos\left(n\frac{y}{R}\right)\sin\left(m\pi\frac{x}{L}\right) \tag{22}$$

where m_a is the added mass due to the fluid contained in the shell, which is given by:

$$m_a = (\rho_F R)\left\{ m\pi\frac{x}{L}\left[\frac{I_{n-1}\left(m\pi\frac{x}{L}\right)}{I_n\left(m\pi\frac{x}{L}\right)} - \frac{nL}{m\pi x}\right]\right\}^{-1} \tag{23}$$

where I_{n-1} and I_n are Bessel functions.

NUMERICAL RESULTS

In this work the following non-dimensional parameters are used:

$$\Gamma_o = \frac{P_0}{P_{cr}} = \frac{R\sqrt{3\left(1-\nu_{SN}^2\right)}}{E_{SN}\,h^2}P_0 \qquad \Gamma_1 = \frac{P_1}{P_{cr}} = \frac{R\sqrt{3\left(1-\nu_{SN}^2\right)}}{E_{SN}\,h^2}P_1 \qquad \Omega = \frac{\omega}{\omega_0} \tag{24}$$

where ω_0 is the fundamental (lowest) natural frequency of the empty shell and $P_{cr} = E\,h^2 \big/ R\sqrt{3\left(1-\nu^2\right)}$ is the static critical load of an axially loaded isotropic cylinder. The critical load of the isotropic silicon nitride shell is used as reference.

Table 1 – Comparison of natural frequencies (Hz) for a empty cylinder and a shell filled with water. (m = 1, L = 0.41 m, R = 0.3015 m, h = 0.001 m, E = 2.1x10^8 kN/m², ν = 0.3, ρ = 7850 kg/m³, ρ_F = 1000 kg/m³).

	Empty Shelll				Fluid-filled			
n	Gasser (1987)	Dym (1973)	Present work	Error (%)	Gasser (1987)	Gonçalves and Batista (1987)	Present work	Error (%)
7	318	305.32	303.35	0.01	-	-	-	-
8	278	281.37	280.94	0.15	120	118	119.2	1.01
9	290	288.28	288.71	0.15	124	124	127.9	3.14
10	334	317.51	318.40	0.28	146	144	146.7	1.87

To check the validity and accuracy of the present methodology for the determination of the natural frequencies, a key point in any non-linear dynamic analysis, empty and fluid-filled cylindrical shells are analyzed and the results are compared with experimental and other numerical values found in literature. As a first example, the lowest natural frequencies of a simply supported empty cylinder are compared with the analytical solution derived by Dym (1973) using Sanders' shell theory and the experimental results obtained by Gasser (1987). The results are shown in Tab. 1. For the same shell, the present results for a water filled shell are compared with those obtained experimentally by Gasser (1987) and the analytical results obtained by Gonçalves and Batista (1987). In both cases, there is an excellent agreement of all results. The error in comparison with the analytical results is rather small.

Consider now a thin-walled cylindrical shell with h = 0.002 m, R = 0.2 m and L = 0.4 m, made of a functionally graded material. The material properties are given in Tab. 2. The damping coefficients, based on experimental results for empty and fluid-filled shells (Pellicano e Amabili 2003), are: ξ = 0.003 (fluid-filled shell), ξ= 0.0008 (empty shell), and η= 0.0001. The fluid mass density is ρ_F=1000kg/m^3 (water).

Table 2. Physical properties of the materials (300 K).

Nickel (Ni)			Silicon Nitride (SN)		
E (N/m²)	ν	ρ (kg/m³)	E (N/m²)	ν	ρ (kg/m³)
205.1 x 10^9	0.31	8900	322.3 x 10^9	0.24	2370

Figure 4 shows the post-buckling behavior of the axially compressed shell for different materials. Increasing the axial load, the shell looses its stability at a sub-critical bifurcation point. The bifurcated solution is unstable up to the fold bifurcation at the minimum post-critical load, when the post-buckling solution becomes stable. Such results show that even if the compression load is much smaller than the critical load, the shell could collapse in the presence of small disturbances. Indeed, considering, the two symmetric branches of the post-buckling path, between the two bifurcation points there are three stable and two unstable solutions. The exponent N defines the gradation of each material through the shell thickness. For comparison purposes, the following limits are considered in this analysis: isotropic silicon nitride shell (N→∞) and isotropic nickel shell (N = 0). Although the material has a measurable influence on the critical load due to variations on the values of the elastic constants, the type of bifurcation and the post-buckling behavior of the shell is not affected by the elastic constants and constitutive law.

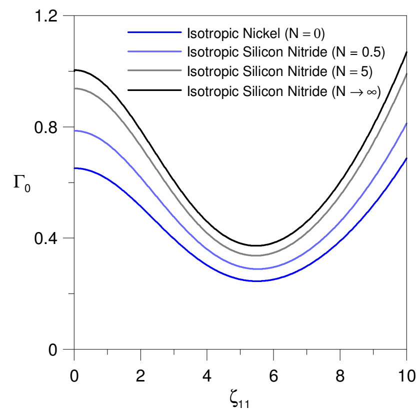

Figure 4 – Post-buckling path of a cylindrical shell with different material gradation exponents.

For this shell geometry, independent of the value of N, the lowest natural frequency occurs for (n, m)=(5, 1) both for empty and fluid-filled shells, as shown in Fig. 5, where the natural frequencies of the shell for m=1 is plotted as a function of n for four different materials. Due to the added mass of the fluid, the natural frequencies decrease without affecting the vibration mode.

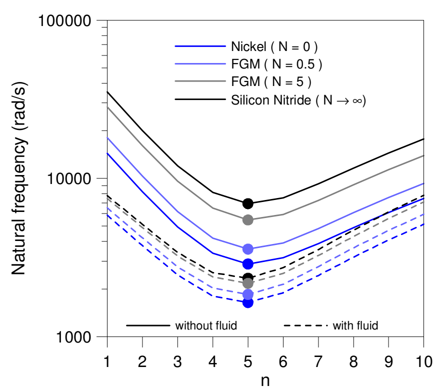

Figure 5 – Variation of the shell natural frequencies as a function of the number of circumferential waves, n, for empty and fluid filled shells considering different constitutive laws (m = 1).

Now the parametric instability and escape from the pre-buckling configuration of the fluid-filled cylinder under axial harmonic forcing, as described by Eq. (4), will be considered. In the following, the constant part of the loading (Γ_0) is assumed to be between the upper and lower static critical load of the shell. In these circumstances, the shell potential energy exhibits three wells, one associated with the fundamental pre-buckling configuration and two wells associated with the two possible post-buckling configurations. If the cylinder is subjected to a periodic axial load, it will undergo the familiar longitudinal forced vibration, exhibiting a uniform transversal motion, due to the effect of Poisson's ratio, also known as breathing mode. However, at certain critical values, the longitudinal motion becomes unstable and the cylinder executes transverse bending vibrations.

Figure 6 shows the numerically obtained parametric instability boundary and escape boundaries for the fluid-filled shell and the same empty shell, in (frequency of excitation x amplitude of excitation) control space for $\Gamma_0 = 0.40$. The lower stability boundary corresponds to parameter values for which small perturbations from the trivial solution will result in an initial growth in the oscillations; therefore it defines the parametric instability boundary. The second limit corresponds to escape from the pre-buckling potential well in a slowly evolving environment. These curves were obtained by increasing slowly the amplitude while holding the frequency constant. As one can observe, the parametric stability boundary is composed of various "curves", each one associated with a particular bifurcation event. The deepest well is associated with the principal instability region at $\omega=2\omega_0$, while the second well to the left is the secondary instability region occurring around $\omega=\omega_0$. The horizontal dotted line corresponds to the static critical load of this shell.

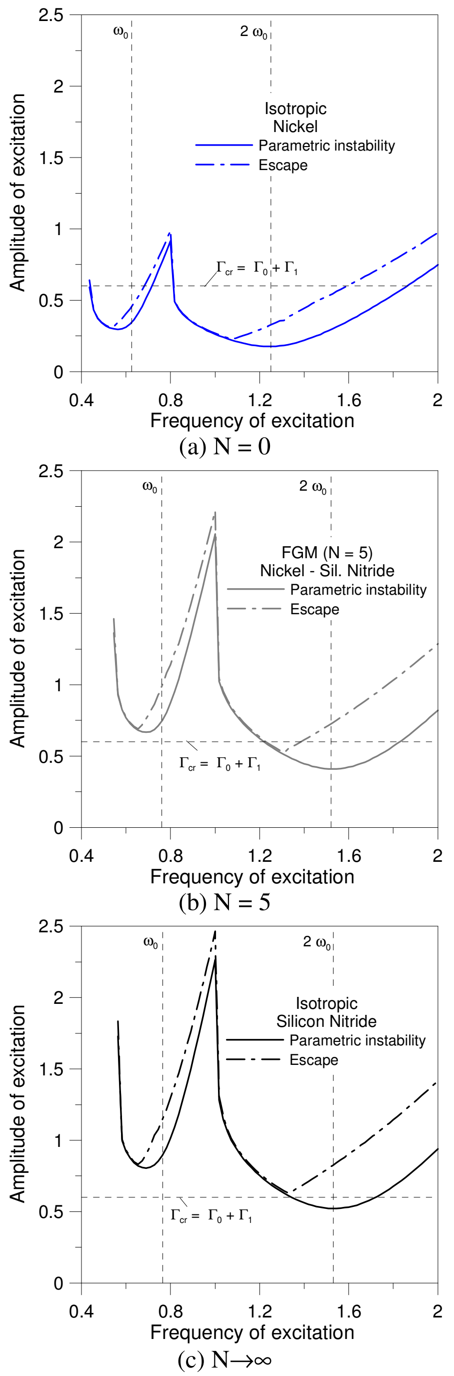

Figure 6 – Stability boundaries in force control space for an empty shell.(Γ_0 = 0.40)

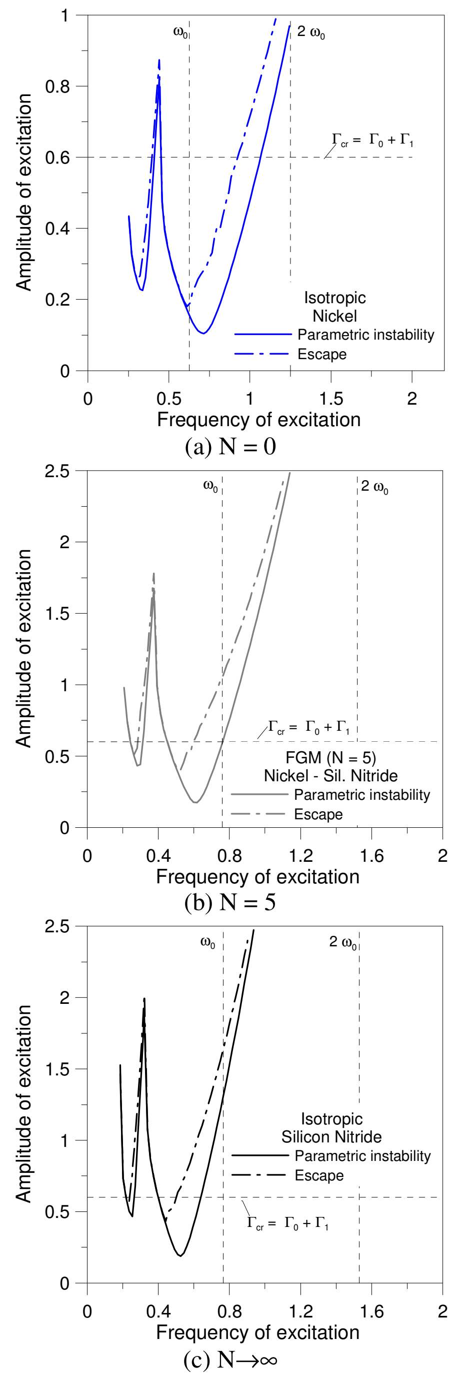

Figure 7 – Stability boundaries in force control space for a fluid-filled shell.(Γ_0 = 0.40)

Comparing Figures 6a – 6c, the stability boundaries shift to the right due to the increase in the gradation exponent N. This is due to the increase in the natural frequency of the shell, as shown in Fig. 5. Also, considering the static pre-stress state constant (Γ_0 = 0.40), the instability boundaries approach the static critical load as N increases from 0 to ∞. The influence of the fluid, in each case, is to shift the stability boundaries to the left due to the added mass, which decreases the natural frequencies. The fluid also causes a decrease in the parametric instability and escape loads, as shown in Figure 7.

The parametric stability boundary for each mode taken separately is composed of various "curves", each one associated with a particular bifurcation event. A detailed parametric analysis indicates that the left hand side of each of these regions is the loci of sub-critical bifurcations, whereas the right hand side is associated with super-critical bifurcations, as illustrated in Figure 8 where bifurcation diagrams of the Poincaré map, obtained by the brute-force method for a given excitation frequency and increasing values of the excitation magnitude, are shown. Neither the gradation exponent nor the fluid alters the type of bifurcation.

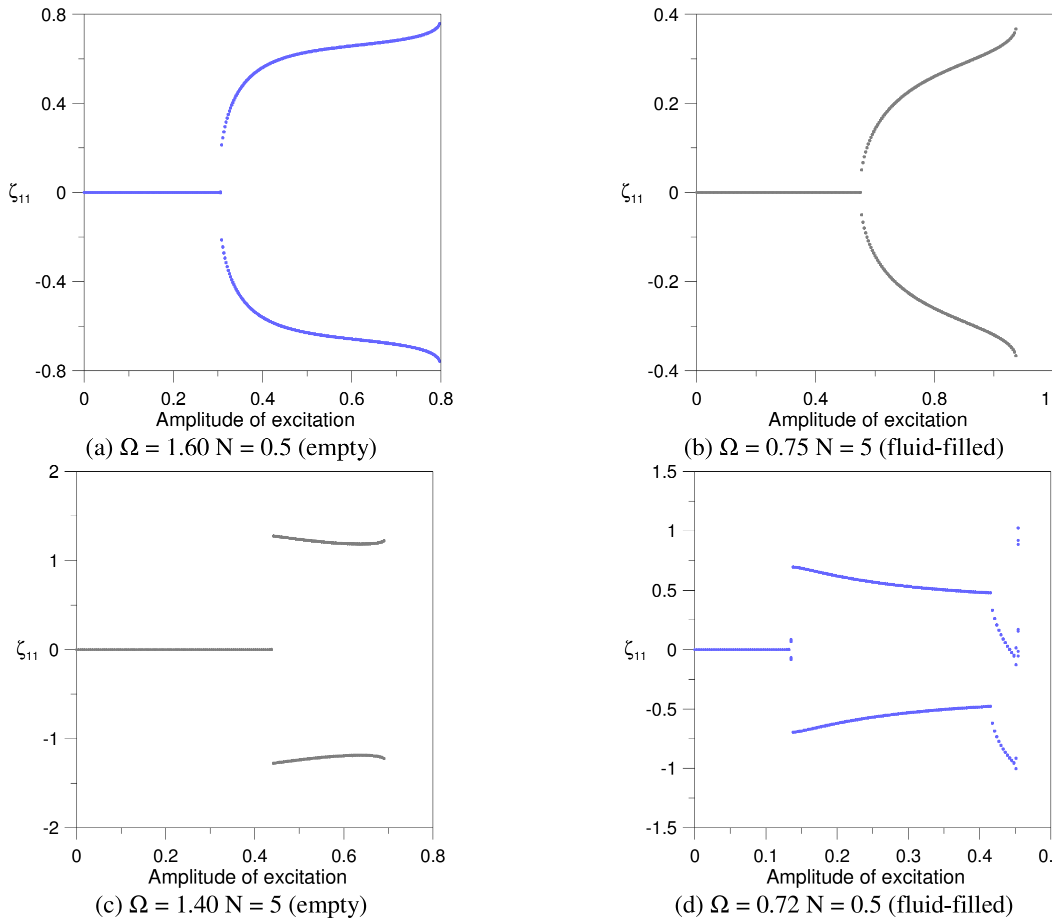

Figure 8 – Bifurcation diagrams for empty and fluid-filled shells.(Γ_0 = 0.40).

CONCLUDING REMARKS

This work presents the nonlinear Donnell shallow shell equations adapted to functionally graded materials with an exponential, smooth variation of the two basic materials through the shell thickness. A modal expansion obtained from a perturbation procedure (Gonçalves and Del Prado, 2002) is used as a basis for the development of a low dimensional model which satisfies the relevant boundary, continuity and symmetry conditions and captures the basic softening behavior exhibited by cylindrical shells. First, this model is used to study the influence of an internal fluid and shell material gradation law on the critical loads and natural frequencies. Then, a detailed parametric analysis is conducted to shown the influence of fluid and shell material on the parametric instability and snap-through buckling of the cylinder. The results show that the fluid-structure interaction leads to a decrease in the buckling loads and a shift of the instability boundaries to a lower frequency region. This is due to the added mass effect of the fluid. The gradation of the material also influences the stability boundaries in force control space. However neither the fluid nor the gradation law has any influence on the softening behavior of the shell or the bifurcation phenomena connected with the instability boundaries.

ACKNOWLEDGMENTS

The authors acknowledge the financial support of the Brazilian research agencies CAPES and CNPq.

REFERENCES

Amabili, M., Sarkar, A., Païdoussis, M. P., 2003, "Reduced-order models for nonlinear vibrations of cylindrical shells via the proper orthogonal decomposition method". Journal of Fluids and Structures, Vol. 18, pp. 227-250.

Dym, C. L., 1973, "Some new results for the vibrations of circular cylinders". Journal of Sound and Vibration, Vol. 29, pp. 189-205.

Gasser, L. F. F, 1987, "Free vibrations of thin cylindrical shells containing fluid (in Portuguese)". Master's Thesis, PEC-COPPE, Federal University of Rio de Janeiro. Rio de Janeiro, RJ, Brazil

Gonçalves, P. B. and Batista, R. C., 1987, "Frequency response of cylindrical shells partially submerged or filled with liquid". Journal of Sound and Vibration, Vol. 113, pp. 59-70.

Gonçalves, P. B. and Batista, R. C., 1988, "Non-Linear Vibration Analysis of Fluid-Filled Cylindrical Shells", Journal of Sound and Vibration, Vol. 127, pp. 133-143.

Gonçalves, P. B. and Del Prado, Z. J. G. N., 2002, "Non-Linear Oscillations and Stability of Parametrically Excited Cylindrical Shells", Meccanica, Vol. 37, pp.569-597.

Hunt, G. W., Williams, K. A. J. and Cowell, R. G., 1986, "Hidden Symmetry Concepts in the Elastic Buckling of Axially Loaded Cylinders", International Journal of Solid and Structures, Vol. 22, pp. 1501-1515.

Koizumi, M., 1997, "FGM activities in Japan", Composites Part B, Vol. 28, pp. 1-4.

Loy, C. T., Lam, K. Y. and Reddy, J. N, 1999, "Vibration of functionally graded cylindrical shells", International Journal of Mechanical Science, Vol. 41, pp. 309-324.

Ng, T. Y., Lam, K. Y., Liew, K. W., and Reddy, J. N., 2001, "Dynamic stability analysis of functionally graded cylindrical shells under periodic axial loading", International Journal of Solids and Structure, Vol. 38, pp.1295-1309.

Pellicano, F. and Amabili, M., 2003, "Stability and vibration of empty and fluid-filled circular cylindrical shells under static and periodic axial loads", International Journal of Solids and Structure, Vol. 40, pp.3229-3251.

Pradhan, S. C., Loy, C. T., Lam, K. Y., and Reddy, J. N., "Vibration characteristics of functionally graded cylindrical shells under various boundary conditions", Applied Acoustics, Vol. 61, pp. 111-129.

Silva, F. M. A., Gonçalves, P. B. and Del Prado, Z. J. G. N., 2006, "Vibrações livres de cascas cilíndricas de material composto com gradação funcional, parcialmente fluid-filleds de fluido". Proceedings of the XXXII Jornadas Sud-Americanas de Ingeniería Estructural, Vol. 1, Campinas-SP, Brazil, pp. 3507-3516.

Sofiyev, A. H., 2005, "The stability of compositionally graded ceramic-metal cylindrical shells under aperiodic axial impulsive loading", Composite Structures, Vol. 69, pp. 247-257.

APPENDIX A

The coefficients A_{ij}, B_{ij} and C_{ij} (i,j = 1,2,6) in equation (7) are given in terms of the elastic constants as:

$$Q_{11} = Q_{22} = \frac{\left[(E_{Ni} - E_{SN})V_{Ni} + E_{SN}\right]}{1 - \left[(\nu_{Ni} - \nu_{SN})V_{Ni} + \nu_{SN}\right]^2} \qquad Q_{12} = \frac{\left[(E_{Ni} - E_{SN})V_{Ni} + E_{SN}\right]\left[(\nu_{Ni} - \nu_{SN})V_{Ni} + \nu_{SN}\right]}{1 - \left[(\nu_{Ni} - \nu_{SN})V_{Ni} + \nu_{SN}\right]^2}$$

$$Q_{66} = \frac{\left[(E_{Ni} - E_{SN})V_{Ni} + E_{SN}\right]}{2\left[1 + (\nu_{Ni} - \nu_{SN})V_{Ni} + \nu_{SN}\right]}$$

$$A_{11} = A_{22} = \int_{-h/2}^{h/2} Q_{11}\, dz \qquad A_{12} = \int_{-h/2}^{h/2} Q_{12}\, dz \qquad A_{66} = \int_{-h/2}^{h/2} Q_{66}\, dz$$

$$B_{11} = B_{22} = \int_{-h/2}^{h/2} Q_{11}\, z\, dz \qquad B_{12} = \int_{-h/2}^{h/2} Q_{12}\, z\, dz \qquad B_{66} = \int_{-h/2}^{h/2} Q_{66}\, z\, dz$$

$$C_{11} = C_{22} = \int_{-h/2}^{h/2} Q_{11}\, z^2\, dz \qquad C_{12} = \int_{-h/2}^{h/2} Q_{12}\, z^2\, dz \qquad C_{66} = \int_{-h/2}^{h/2} Q_{66}\, z^2\, dz$$

RESPONSIBILITY NOTICE